

Hierarchical crystal growth of sheaf-like CdS by microemulsion/hydrothermal route

Maryam Mohammadikish¹ · Haneih Hajisadeghi¹

Received: 21 June 2016 / Accepted: 2 September 2016 / Published online: 7 September 2016
© Springer Science+Business Media New York 2016

Abstract Cadmium sulfide nanostructures with a sheaf-like morphology were obtained via the simple microemulsion/hydrothermal process. By controlling the synthetic parameters such as reaction time, temperature and microemulsion media, different morphologies were obtained. These new CdS structures were characterized by X-ray diffraction (XRD), Fourier transform infrared spectroscopy (FT-IR) and scanning electron microscopy (SEM). The optical properties of CdS semiconductor were discussed by the UV–Vis absorption and photoluminescence (PL) studies. Sheaf-like structures may be formed by the splitting crystal growth mechanism, which is known to explain the morphology of some mineral crystals present in nature.

1 Introduction

Monodisperse and small particles of semiconductors have received impressive attention in recent years because of the expectation of optical and electronic properties [1–3]. This increasing interest has led to a wide range of preparative approaches to nanostructures. The key point to any synthetic investigation must be a careful control of the size and size-distribution of particles.

Cadmium sulfide, as one of the most technologically important class of materials, is a *n*-type semiconductor with wide band gap of 2.42 eV at room temperature. In CdS nanocrystals, which demonstrate properties between the molecular and bulk limits, a number of striking effects such

as nonlinear optical behaviors, size quantization, fluorescence and solar cell application have been explored [4–7].

Various methods such as hydrothermal [8, 9], microwave-solvothermal synthesis [10, 11], thermal decomposition [12], laser irradiation synthesis [13], ionic liquid-assisted synthesis [14], and surfactant-assisting solvothermal method [15] used to synthesize nano and micro-crystalline CdS. Most of the products have different morphologies such as nanowires [16–18], nanorods [15, 19, 20], dendrites [21], spheres [9, 22], flakes [23], triangular and hexagonal plates [24], sea-urchin-like shape [25] and flower-like shape [26].

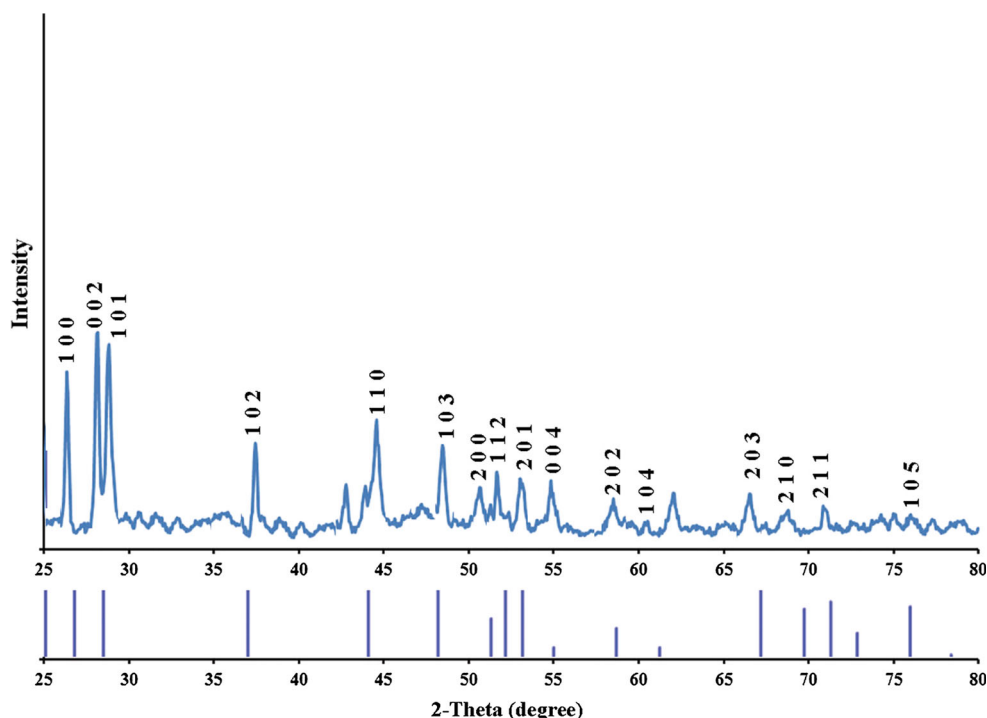
Compared with nanoparticles, the preparation and study of nanorods and nanoplates as building blocks for hierarchically structures are of considerable interest because of their special properties and wide applications in nanodevices [27, 28]. Since many fundamental properties of semiconductor materials have been expressed as a function of the size and shape, the control of nucleation and growth of nanostructural materials is becoming critical, which can provide opportunities of tailoring properties of materials and offer possibilities for observing interesting physical phenomena [29].

It is well known that microemulsions are one of the effective media to prepare nanoparticles [30–32]. In water-in-oil microemulsions nano-sized water droplets were surrounded by surfactants to form reversed micelles and steadily disperse into the oil phase. They provide the ideal environment for the preparation of nanoparticles since water droplets represent nanoreactors which favor the formation of small crystallites with a narrow size distribution. When microemulsions were combined with hydrothermal treatment, the crystallinity of the product would be improved greatly. The hydrothermal process has been employed to control the nucleation and growth of CdS crystals or as a treatment of microemulsions to improve the crystal phase

✉ Maryam Mohammadikish
mohammadikish@khu.ac.ir

¹ Faculty of Chemistry, Kharazmi University, Tehran, Iran

Fig. 1 XRD pattern of the CdS prepared in isooctane/water/PEG/1-propanol microemulsion at 180 °C for 6 h



[33, 34]. The quaternary microemulsion of isooctane/polyethyleneglycole (PEG)/1-propanol/water, a typical reaction media for nanocrystals [35], were applied here.

The crystal growth of CdS is also determined by mass transport process via control of decomposition rate of free S^{2-} from the sulfur source in the solution [36]. However, to the best of our knowledge, a general route for the synthesis of CdS sheaf-like structures under microemulsion-hydrothermal conditions with thioglycolic acid as sulfur source has still not been realized. This work presents a novel microemulsion-hydrothermal technique to synthesize uniform sheaf-like structures of cadmium sulfide clusters. The composition, microstructure, optical properties and formation mechanism of the obtained nanocrystals are characterized in detail.

2 Experimental

2.1 Materials and equipments

All chemicals were of analytical grade and were used as received without further purification. XRD patterns were recorded by a Rigaku D-max C III, X-ray diffractometer using Ni-filtered $Cu K\alpha$ radiation. Scanning electron microscopy (SEM) images were obtained on KYKY-EM3200. Fourier transform infrared (FT-IR) spectra were recorded on Perkin-Elmer Spectrum RXI FT-IR spectrometer in KBr pellets. The electronic spectra of the complexes were taken on a Perkin-Elmer lambda 25

spectrometer. Photoluminescence (PL) measurements were carried out on a Perkin-Elmer LS-55 luminescence spectrometer using a pulsed Xe lamp.

2.2 Preparation of CdS nanocrystals

In a typical experimental procedure, 1.75 mL aqueous solution of cadmium acetate (1 mol/L) was added with vigorous stirring to 4.75 mL isooctane as oil, 0.75 mL PEG (polyethylene glycol 200) as surfactant and 9 mL 1-propanol as co-surfactant to form quaternary microemulsion system. After the microemulsion became transparent, 1 mL aqueous solution of thioglycolic acid (5.6 mol/L) was added to the mixture. A milky white solution was formed immediately after addition of TGA that was transferred into a Teflon-lined stainless steel autoclave and kept at 180 °C for 6 h. Finally, the autoclave was cooled to room temperature naturally. The yellow precipitate was obtained by centrifugation and washed with distilled water and ethanol several times. Various times, temperatures and microemulsion media were investigated to evaluate the effect of these parameters on the morphologies of the products.

3 Results and discussions

3.1 X-ray diffraction analysis

The XRD pattern in Fig. 1 shows that the as-prepared CdS sample at 180 °C-6 h is in the hexagonal phase with lattice

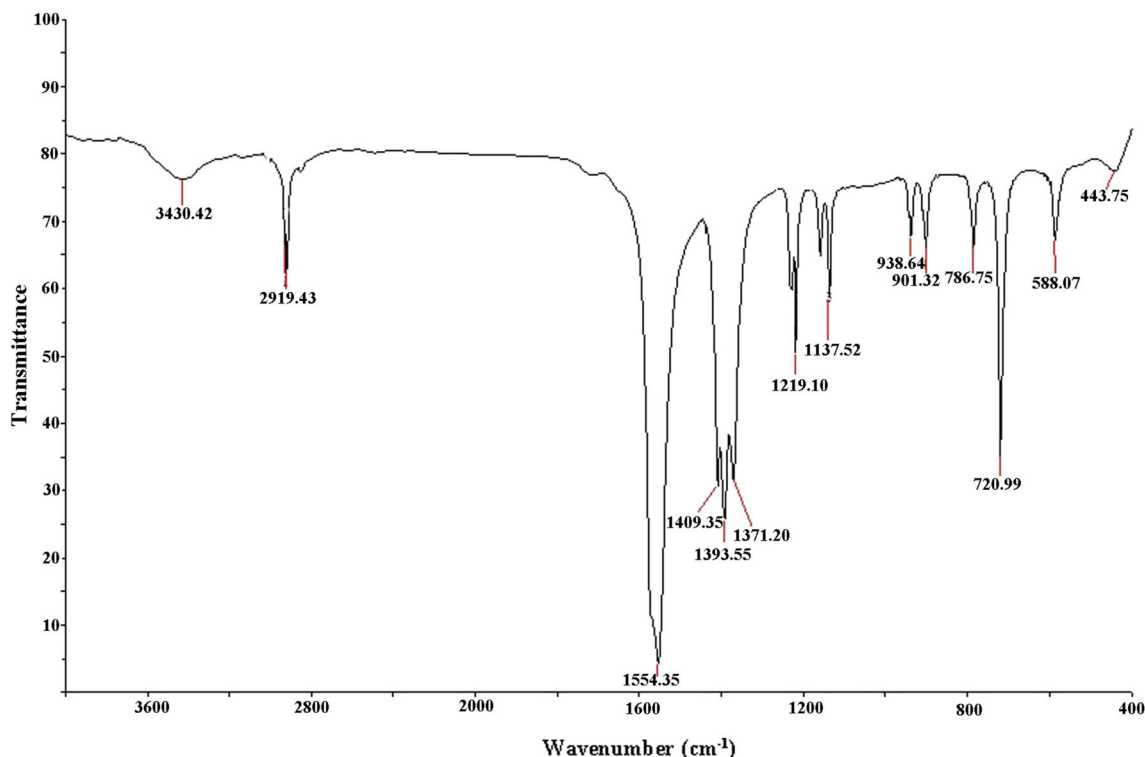


Fig. 2 FT-IR spectrum of the CdS prepared in isooctane/water/PEG/1-propanol microemulsion at 180 °C for 6 h

constants consistent with the values in the literature (JCPDS Card, File No. 77-2306). The XRD pattern confirms the *wurtzite* crystal structure with *P63mc* space group. According to Rhee et al. the temperature at which CdS nanocrystals changes from the amorphous phase to the hexagonal phase when treated with the hydrothermal method was up to 160 °C, and a nearly complete hexagonal phase was obtained at 240 °C [37]. The higher intensity of the (0 0 2) peak indicates that the crystals are grown along the *c*-axis, which suggests that the [001] direction was aligned along the nanorod axis of the CdS nanocrystals. It is interesting to observe that the reported CdS nanorods with the strongest intensity of the (002) diffraction peak have the same preferential orientation along the *c* axis [38, 39]. The rod-like shape is confirmed by SEM photographs that will be discussed later.

3.2 Fourier transform infrared spectroscopy

To investigate whether the surface of the samples was capped with organic materials the Fourier transformed infrared (FT-IR) spectra of the as-synthesized samples were recorded. Figure 2 shows typical FT-IR spectrum of CdS nanocrystals prepared at 180 °C for 6 h. The peak at 3430 cm⁻¹ could be due to the adsorption of H₂O in the sample. The absorption peaks at 2931 and 2919 cm⁻¹ can be ascribed to asymmetric (ν_{as}) and symmetric stretching

vibration (ν_s) of the CH₂ groups, respectively. The relatively strong absorption peaks at 1555 cm⁻¹ and another at 1394 cm⁻¹ could be assigned to the C = O asymmetric (ν_{as}) and symmetric stretching vibrations (ν_s), respectively. From the IR spectra, carboxylates are confirmed to be present in the as-obtained products. An absorption band due to S–H vibration at 2500–2600 cm⁻¹ is absent. Therefore, these results strongly suggest that the thiol groups of TGA coordinate with Cd²⁺ ions on the CdS surface.

From the results of FT-IR analysis, it is suggested that the organic component –CH₂COOH should exist in the composite. It is believed that these absorption peaks are close to those of (CdS)_{*m*}(CdSCH₂COOH)_{*k*}²⁺ [30]. Furthermore, a blue shift of the Cd–S stretching vibration was observed from 803 to 720 cm⁻¹ [40, 41]. This can be attributed to the interaction of the TGA with the CdS molecules.

3.3 Scanning electron microscopy

The typical morphology and structure of CdS were characterized by scanning electron microscopy (SEM). Figure 3 shows that the as-prepared CdS nanocrystals have sheaf-like 3D architectures with highly self-assembled hierarchical and repetitive super-structures. When the reaction was carried for 6 h at 120 °C (Fig. 3a, b), a large number of CdS sheaf-like structures were formed as shown

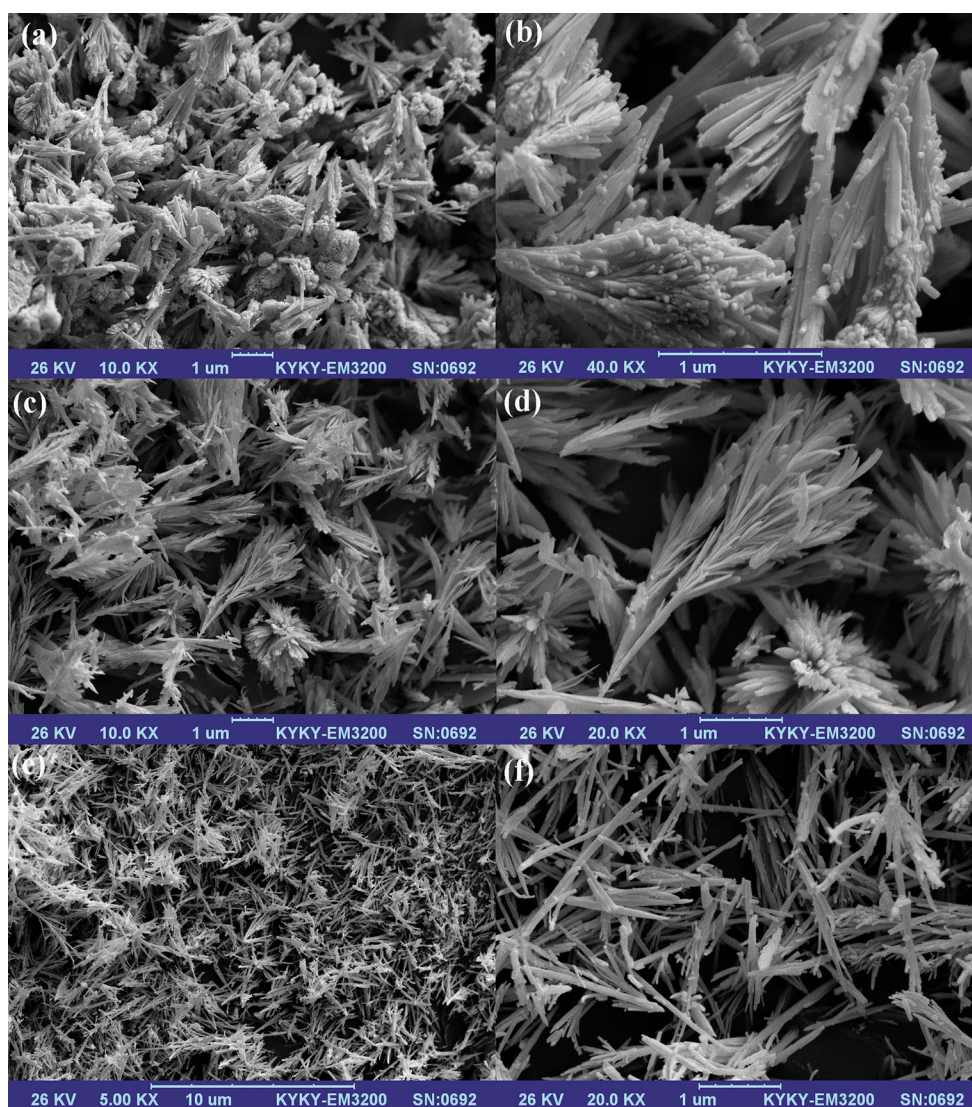


Fig. 3 SEM images of CdS nanostructures synthesized in isooctane/water/PEG/1-propanol microemulsion for 6 h at (a, b) 120 °C, (c, d) 150 °C, and (e, f) 180 °C

in Fig. 3a. More detailed morphologies as shown in Fig. 3b display that several dozens of nanoribbons with thickness of 20–30 nm connect to each other forming 3D sheaf-like structures by self-assembly process. Also, some tiny nanoparticles on the surface of the nanoribbons can be seen. With increasing reaction temperature to 150 °C, sheaf-like structures consisting of ordered nanoribbons with increasing thickness to 40–50 nm were obtained (Fig. 3c, d). No nanoparticles were existed on the surface of nanoribbons in this temperature. With increasing the reaction temperature to 180 °C, the morphologies of the products change from complex sheaf-like super-structures to simple nanorods with thickness of about 45 nm.

The influence of the time on the morphology of products was studied at 180 °C. After 15 h of solvothermal treatment, some 1D thin nanorods surrounded by a large

amount of nanoparticles came out in the products as shown in Fig. 4a, b. By further prolonging the reaction time to 18 h, the amount of nanoparticles increased at the expense of the nanorods (Fig. 4c, d). In this formation process, time was the most important controlling factor.

As a control experiment, the microemulsion media was changed. In the new microemulsion system comprised of H₂O (3 mL), cyclohexane (7 mL), Triton-X-100 (2 mL) and 2-propanol (8 mL), at 180 °C for 6 h, nanorods surrounded by a large amount of nanoparticles were formed again (Fig. 5a). The XRD pattern of this composite (Fig. 5b) showed characteristic peaks of wurtzite structure of CdS. This experiment showed that the change in microemulsion media have no effect on the morphology of the products, while the time and temperature of hydrothermal process are the important factors.

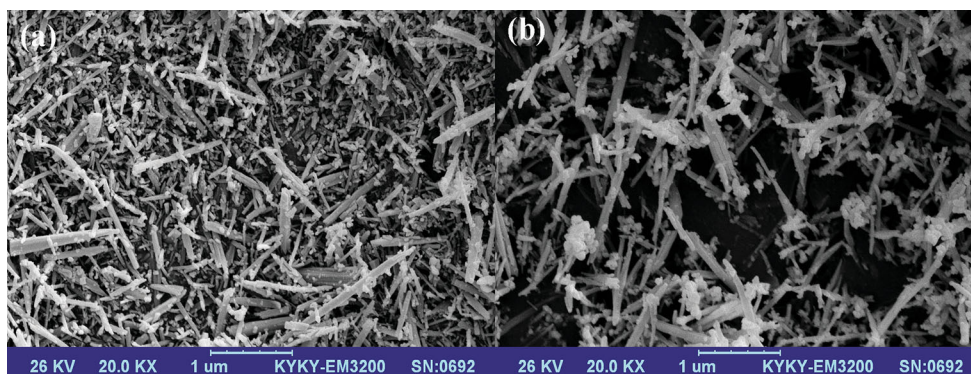


Fig. 4 SEM images of CdS nanorods synthesized in isooctane/water/PEG/1-propanol microemulsion at 180 °C for **a** 15 h, and **b** 18 h

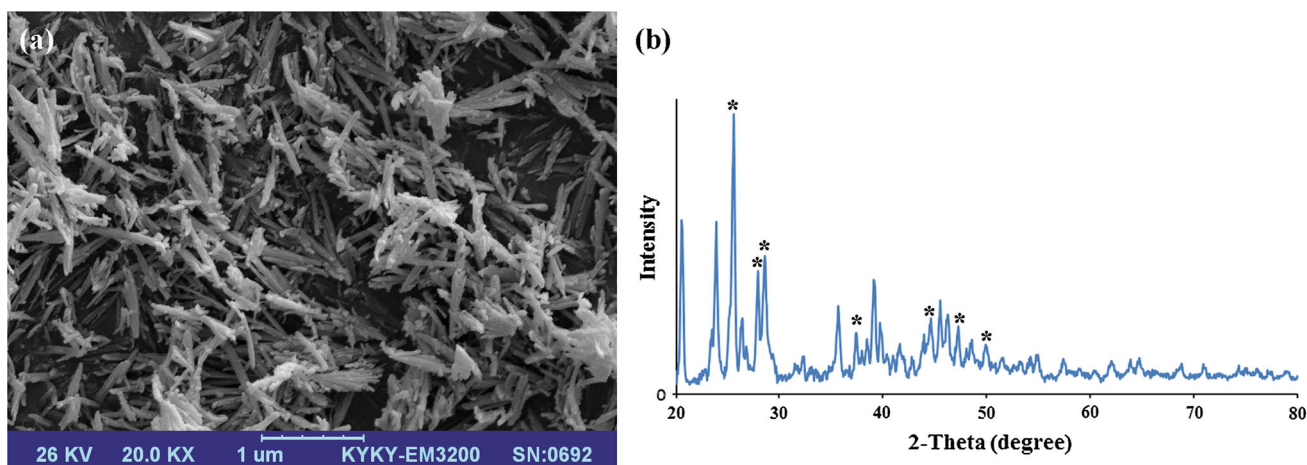
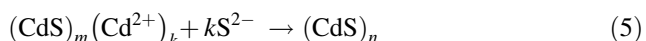
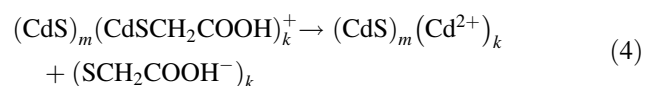
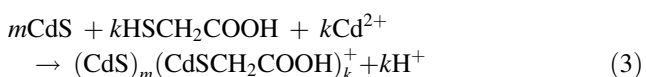


Fig. 5 **a** SEM image and **b** XRD pattern of CdS nanocrystals synthesized in H₂O/cyclohexane/Triton-X-100/2-propanol microemulsion at 180 °C for 6 h

3.4 Growth mechanism

Because of slow dissociation of S²⁻ from TGA, the complex CdS clusters, (CdS)_m(CdSCH₂COOH)_k⁺, was formed according the following equation [36]:



Prior to the hydrothermal process, the reactions (1–3) have taken place, the (CdS)_m(CdSCH₂COOH)_k⁺, i.e., the complex CdS clusters are the major species in the solution, manifested by the milk white solution as mentioned in experimental part.

The reactions 4–5 took place during the hydrothermal process. Reaction (4) illustrates the dissociation of the complex CdS clusters. Therefore, during the hydrothermal process, the formation of CdS precedes along the specific directions, dependent on the status of SCH₂COOH⁻ dissociation from the complex CdS cluster.

Very interestingly, it has already been found that some minerals tend to grow into this seemingly unusual sheaf-like structure in nature. It is believed by mineralogists that the sheaf structures may be formed by crystal splitting during their growth. Successive stages of splitting during crystal growth are shown in Fig. 6. An individual crystal splits formed a number of sub-individuals (simple splitting), a sheaf-like structure [42].

It is found that, by controlling the temperature, various morphologies of CdS can be obtained. The degree of crystal splitting decreases with increasing temperature, i.e., from sheaf-like structures at 120 °C (Fig. 3a, b) to nanoribbon bundles, with simple splitting or individual nanorods with no splitting, at 180 °C (Fig. 3e, f). These

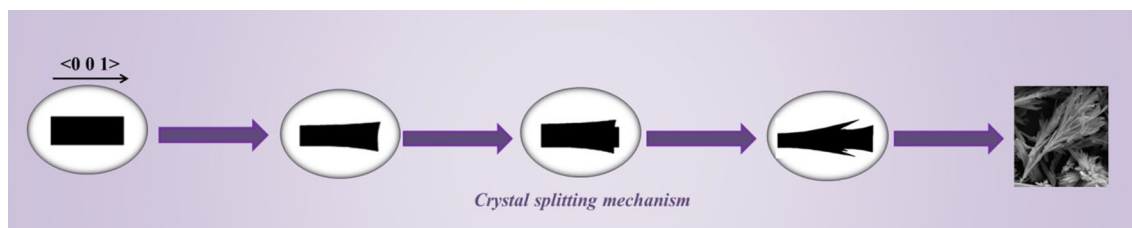


Fig. 6 Schematic illustration of the successive stages of splitting during crystal growth

observations may be explained in the crystal-splitting theory in conjunction with the nucleation and growth theory of nanocrystals. At higher temperatures, more nuclei will form in a shorter time and a large number of nuclei will then grow slowly.

The sheaf-like CdS reported here splits not only from the stem, but also from the branches into fine nanoribbons. As is known, splitting in crystal growth is associated with both kinetic and thermodynamic factors: fast crystal growth [35] and extramolecules appearing in the parent solution [36].

3.5 Optical properties of CdS

The optical properties of CdS were characterized by UV/vis absorption and photoluminescence (PL) spectroscopy. To examine the quantum-confined effect of the product, room-temperature UV–vis absorption spectra of the CdS, which were dispersed in water, were recorded. Figure 7 shows the UV–vis absorption spectra of the CdS sample obtained at 180 °C for 6 h. This sample displays a broad absorption peak centered at about 460 nm. The peak shows a blue shift with respect to bulk CdS (515 nm) [43, 44]. This point suggests that the as-synthesized CdS are formed of nanostructures and are assembled of nano-sized particles, which is in consistency with the SEM images.

There is a very small red-shift relative to that of nano-sized CdS when compared to the previous reports [45, 46] where it is considered that the smaller nanoparticles are restricted in micron-sized structure assemblies.

Moreover, the optical band gap of the as-prepared samples was evaluated from the absorption spectrum using the Tauc relation [47, 48].

$$(\epsilon hv) = C (hv - E_g)^n \quad (6)$$

where C is a constant, ϵ is the molar extinction coefficient, E_g is the average band gap of the material and n depends on the type of transition. For $n = 1/2$, E_g in Eq. (6) is the direct allowed band gap. The average band gap was estimated from the linear portion of the $(\epsilon hv)^2$ vs. hv plots (Fig. 7b). The band gap value was higher than the value of

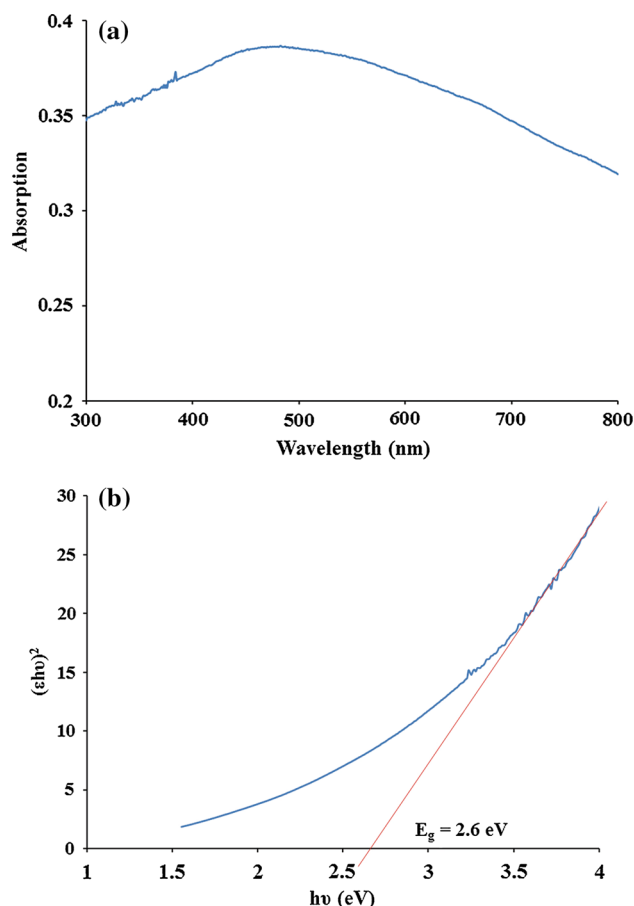


Fig. 7 **a** UV–Vis spectrum and **b** tauc plot of the as-prepared CdS sample synthesized in isoctane/water/PEG/1-propanol microemulsion at 180 °C for 6 h

bulk CdS (2.42 eV) [30, 40] due to quantum confinement of CdS nanoparticles.

Figure 8 shows the PL spectrum of the as-prepared sheaf-like CdS sample obtained at 180 °C for 6 h. The luminescence spectrum is excited with 420 nm photons and emission peak at about 543 nm. It presents some blue-shift compared to bulk CdS at 650 nm [49], which is consistent with the result of above UV–vis absorption spectrum. Calculated band gap from this spectrum is in good accordance (2.7 eV) with the results in UV–vis

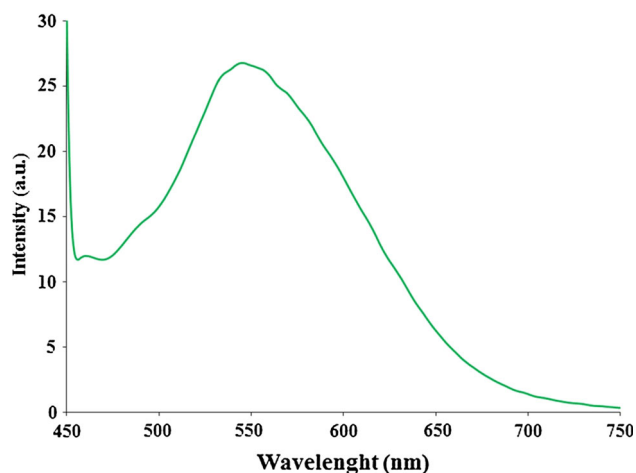


Fig. 8 Room temperature photoluminescence spectra of the as-prepared CdS sample synthesized in isoctane/water/PEG/1-propanol microemulsion at 180 °C for 6 h

spectra. The apparent blue shift and the strong peak also indicatives of the size quantization of as-prepared CdS nanostructures.

4 Conclusions

In summary, novel 3D sheaf-like CdS nanostructures have been synthesized in a mild isoctane/PEG/1-propanol/water microemulsion system under hydrothermal conditions. The crystal splitting mechanism was used to explain the formation of sheaf-like structures. It has been found that both the reaction time and temperature play important roles in the growth of the final morphology. Our results demonstrate that microemulsion-based hydrothermal approach provides a new chemical route to inorganic 3D complex structures, which may find applications in many technological fields. Band gaps of CdS as-prepared nanostructures were calculated by UV–vis and PL spectra is 2.6 eV which showed 0.2 eV blue shift in comparison to bulk CdS band gap.

Acknowledgments The authors are grateful to Kharazmi University for financial support.

References

1. F. Davar, M. Mohammadikish, M.R. Loghman-Estarki, M. Masteri-Farahani, Synthesis of micro- and nanosized PbS with different morphologies by the hydrothermal process. *Ceram. Int.* **40**, 8143 (2014)
2. M. Mohammadikish, F. Davar, M.R. Loghman-Estarki, Various morphologies of nano/micro PbS via green hydrothermal method. *J. Mater. Sci.: Mater. Electron.* **26**, 2937 (2015)
3. M. Mohammadikish, H. Hajisadeghi, Synthesis and growth mechanism of CdO nanoparticles prepared from thermal

decomposition of CdSO₃ nanorods. *J. Mater. Sci.: Mater. Electron.* **27**, 6480 (2016)

4. O. Amiri, M. Salavati-Niasari, S.M. Hosseinpour-Mashkani, A. Rafei, S. Bagheri, Cadmium selenide@sulfide nanoparticle composites: facile precipitation preparation, characterization, and investigation of their photocatalyst activity. *Mater. Sci. Semicond. Proc.* **27**, 261 (2014)
5. M. Sabet, M. Salavati-Niasari, O. Amiri, Using different chemical methods for deposition of CdS on TiO₂ surface and investigation of their influences on the dye-sensitized solar cell performance. *Electrochim. Acta* **117**, 504 (2014)
6. V.A. Fokerov, E.P. Pokatilov, V.M. Fomin, J.T. Devreese, V.A. Fokerov, E.P. Pokatilov, V.M. Fomin, J.T. Devreese, *Phys. Rev. Lett.* **92**, 127402 (2004)
7. E. Esmaeili, M. Sabet, M. Salavati-Niasari, Z. Zarghami, S. Bagheri, Effect of sulfur source on cadmium sulfide nanostructures morphologies via simple hydrothermal route. *J. Cluster Sci.* **27**, 351 (2016)
8. M. Salavati-Niasaria, M.R. Loghman-Estarkia, F. Davar, Controllable synthesis of nanocrystalline CdS with different morphologies by hydrothermal process in the presence of thioglycolic acid. *Chem. Eng. J.* **145**, 346 (2008)
9. X. Li, B. Yang, Y. Yang, Y.T. Qian, *J. Cryst. Growth* **291**, 45 (2006)
10. Z. Yu, B. Yin, F. Qu, X. Wu, *Chem. Eng. J.* **258**, 203 (2014)
11. A.V. Murugan, R.S. Sonawane, B.B. Kale, S.K. Apte, A.V. Kulkarni, *Mater. Chem. Phys.* **71**, 98 (2001)
12. J.F.A. Oliveira, T.M. Milao, V.D. Araujo, M.L. Moreira, E. Longo, M.I.B. Bernardi, *J. Alloy. Compd.* **509**, 6880 (2011)
13. D.C. Onwudiwe, C.A. Strydom, *Spectrochim. Acta A* **135**, 1080 (2015)
14. D.C. Onwudiwe, T.P.J. Krüger, O.S. Oluwatobi, C.A. Strydom, *Appl. Surf. Sci.* **290**, 18 (2014)
15. K. Yao, W. Lu, J. Wang, *Mater. Chem. Phys.* **130**, 1175 (2011)
16. C. Bao, M. Jin, R. Lu, P. Xue, Q. Zhang, D. Wang, Y. Zhao, *J. Solid State Chem.* **175**, 322 (2003)
17. C. Cheng, G. Xu, H. Zhang, H. Wang, J. Cao, H. Ji, *Mater. Chem. Phys.* **97**, 448 (2006)
18. X. Guo-Yue, W. Han, C. Chuan-Wei, Z. Hai-Qian, C. Jie-Ming, J. Guangbin, *Trans. Nonferrous Met. Soc. China* **16**, 105 (2006)
19. C.J. Barrelet, Y. Wu, D.C. Bell, C.M. Lieber, *J. Am. Chem. Soc.* **125**, 11498 (2003)
20. W. Qingqing, Z. Gaoling, H. Gaorong, *Mater. Lett.* **59**, 2625 (2005)
21. Y.D. Li, H.W. Liao, Y.T. Qian, L. Yang, G.E. Zhou, *Chem. Mater.* **10**, 2301 (1998)
22. A.M. Qin, Y.P. Fang, W.X. Zhao, H.Q. Liu, C.Y. Su, *J. Cryst. Growth* **283**, 230 (2005)
23. F.H. Zhao, Q. Su, N.S. Xu, C.R. Ding, M.M. Wu, *J. Mater. Sci.* **41**, 1449 (2006)
24. N. Gao, F. Guo, *Mater. Lett.* **60**, 3697 (2006)
25. M. Chen, L. Pan, J. Cao, H. Ji, G. Ji, X. Ma, Y. Zheng, *Mater. Lett.* **60**, 3842 (2006)
26. X. Liu, *Mater. Chem. Phys.* **91**, 212 (2005)
27. L. Wang, L. Chen, T. Luo, Y. Qian, *Mater. Lett.* **60**, 3627 (2006)
28. G. Fasol, *Science* **280**, 545 (1998)
29. Y.D. Li, H.W. Liao, Y. Ding, Y. Fan, Y. Zhang, Y.T. Qian, *Inorg. Chem.* **38**, 1382 (1999)
30. J. Yang, J.H. Zeng, S.H. Yu, L. Yang, G.E. Zhou, Y.T. Qian, *Chem. Mater.* **12**, 3259 (2000)
31. M. Masteri-Farahani, H.S. Hosseini, *Powder Technol.* **228**, 228 (2012)
32. M. Masteri-Farahani, S. Mahdavi, M. Rafizadeh, *Ceram. Int.* **39**, 4619 (2013)
33. M. Masteri-Farahani, M. Sadrinia, *Powder Technol.* **217**, 554 (2012)

34. S.J. Xu, S.J. Chua, B. Liu, L.M. Gan, C.H. Chew, G.Q. Xu, *Appl. Phys. Lett.* **73**, 478 (1998)
35. W.W. So, J.S. Jang, Y.W. Rhee, K.J. Kim, S.J. Moon, *J. Colloid Interface Sci.* **237**, 136 (2001)
36. Z. You, I. Balint, K. Aika, *App. Catal B* **53**, 233 (2004)
37. H. Zhang, D. Yang, X. Ma, Y. Ji, S.Z. Li, D. Que, *Mater. Chem. Phys.* **93**, 65 (2005)
38. W.W. So, J.S. Jang, Y.W. Rhee, K.J. Kim, S.J.J. Moon, *Colloid Interface Sci.* **237**, 136 (2001)
39. M. Chen, Y. Xie, J. Lu, Y. Xiong, S. Zhang, Y. Qian, X. Liu, *J. Mater. Chem.* **12**, 748 (2012)
40. H. Zhang, X. Ma, Y. Ji, J. Xu, D. Yang, *Chem. Phys. Lett.* **377**, 654 (2003)
41. D. Jiang, L. Ding, J. Huang, E. Gu, L. Liu, Z. Chai, D. Liu, *Polymer* **48**, 7156 (2007)
42. B.T. Raut, M.A. Chougule, S.R. Nalage, D.S. Dalavi, S. Mali, P.S. Patil, V.B. Patil, *Ceram. Int.* **38**, 5501 (2012)
43. Y. Hu, K. Chen, *J. Cryst. Growth* **308**, 185 (2007)
44. Z.H. Zhang, W.S. Chin, J.J. Vittal, *J. Phys. Chem. B* **108**, 18569 (2004)
46. S.H. Hwang, C.N. Moorefield, P. Wang, K.U. Jeong, S.Z.D. Cheng, K.K. Kotta, G.R. Newkome, *Chem. Commun.* **33**, 3495 (2006)
46. J. Jang, S. Kim, K.J. Lee, *Chem. Commun.* **26**, 2689 (2007)
47. K.T. Yong, Y. Sahoo, M.T. Swihart, P.N. Prasad, *J. Phys. Chem. C* **111**, 2447 (2007)
48. J. Tauc, in *Optical Properties of Solids*, ed. by F. Abeles (North-Holland, Amsterdam, 1970)
49. A. Kumar, V. Kumar, *J. Phys. Chem. C* **112**, 3633 (2008)